THIN-FILM MICROSTRIP LINES FOR MM AND SUB-MM-WAVE ON-CHIP INTERCONNECTS

H.-M. Heiliger[a)], M. Nagel, H. G. Roskos[b)], and H. Kurz
Institut für Halbleitertechnik II, Rheinisch-Westfälische Technische Hochschule (RWTH) Aachen, Sommerfeldstraße 24, D-52056 Aachen, Germany

F. Schnieder and W. Heinrich
Ferdinand-Braun-Institut für Höchstfrequenztechnik Berlin, Rudower Chaussee 5, D-12489 Berlin, Germany

ABSTRACT

Thin-film microstrip lines with a polymer dielectric between ground and signal conductor are proven to be an attractive alternative to coplanar waveguides for (sub)-mm-wave interconnects. Both simulation and electrooptic characterization reveal negligible modal dispersion up to 1000 GHz and low attenuation even if the lines are realized on low-resistivity sustrates.

INTRODUCTION

The growing number of mm and sub-mm-wave applications demands solutions for the monolithic implementation of high-speed circuits. Regarding the transmission-line types in use, commonly the coplanar waveguide (CPW) design concept is preferred over microstrip line (MSL) approaches for the following reasons. For conventional MSLs with 50 Ω impedance, the signal-conductor width has to be in the same order of magnitude as the substrate thickness, i.e., it is relatively large compared to the CPW dimensions. As a consequence, modal dispersion (e.g. [1]) increases and makes conventional MSLs unsuitable for applications in the (sub)-mm-wave range. CPWs, however, also do not represent ideal solutions, since scaling down the dimensions results in relatively high attenuation due to metallic losses.

An attractive alternative is the thin-film microstrip line (TFMSL) with characteristic dimensions in the micron range while maintaining the standard 50 Ω characteristic impedance level [1,2]. For this type of line, both ground and signal conductor are located on top of the substrate separated by a suitable dielectric. Thus, the width of the signal line and the height of the dielectric, respectively, can be freely chosen within a wide range. Additionally, the shielding effect of the ground metallization decouples the fields from the substrate. This decoupling appears particularly important when low-resistivity semiconductor substrates are in use.

So far, no systematic comparison between the different line types has been made. This is the purpose of our paper where method-of-lines (MoL [3]) simulations and electrooptic measurements on TFMSLs are presented and compared with CPW properties.

THE THIN-FILM MICROSTRIP LINE (TFMSL)

The TFMSLs, as sketched in Fig. 1, are prepared on low-resistivity (5-8 Ωcm) Si substrates. They consist of a 800-nm-thick Al ground conductor and a 800-nm-thick and 8-μm-wide Al signal conductor including a 5-μm-long photoconductive (PC) gap for generation of ps electric pulses directly on the line. The PC gap is based on lift-off low-temperature-grown GaAs (LT-GaAs). Either SiO_2 or BCB (bisbenzocyclobutene) is used as dielectric between both conductors.

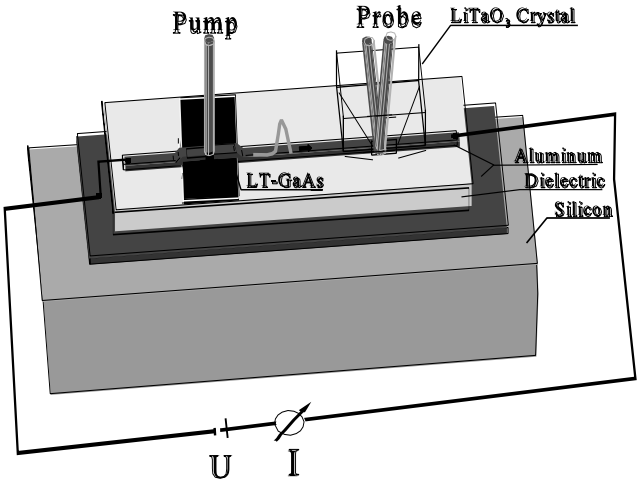

FIG. 1: Schematic illustration of the TFMSL and the experimental setup for picosecond electric pulse generation and electrooptic on-wafer measurement.

In order to obtain structures with an integrated PC switch, small samples ($0.5 \cdot 0.5$ mm^2) of 500-nm-thick LT-GaAs are lifted from the original substrate and bonded onto the dielectric following the procedure described in [4]. The PC material is grown by molecular beam epitaxy on (100)-oriented semi-insulating GaAs. The epitaxial layers consist of 100 nm sacrificial AlAs deposited at 550°*C* and the 500-nm-thick LT-GaAs film grown at 200°*C* and annealed in situ at 615°*C* for 15 min in an As-rich atmosphere. In order to minimize the influence of the bonded semiconductor on the line properties,

0-7803-4603-6/97/$5.00 (c) IEEE

the LT-GaAs is patterned into 20-μm-wide stripes by wet chemical etching using a photoresist as etching mask. After removal of the resist, the signal conductor with a 5 μm gap on top of the LT-GaAs (compare Fig.1) is prepared by means of conventional lift-off technique. Both the signal and ground metallization layers are deposited by electron-beam evaporation.

TIME-DOMAIN MEASUREMENTS - FREQUENCY-DOMAIN ANALYSIS

The TFMSLs are characterized by time-domain electrooptic sampling [5] (see Fig.1) employing 150-fs optical pulses from a 76-MHz Ti:Al_2O_3 laser operating at a wavelength of 750 nm. The laser beam is split into two parts by a polarizing beam splitter. The pump beam (4 mW average power) illuminates the 15-V-biased PC gap within the TFMSL generating ps electric pulses. The time-delayed probe pulses detect the electric transients after a propagation distance z_k with the help of a $LiTaO_3$ electooptic transducer. A lock-in detection scheme reduces the noise level.

The complex propagation constant $\gamma(f) = \alpha(f) + i \cdot \beta(f)$, with $\alpha(f)$ describing the frequency-dependent attenuation and $\beta(f)$ the phase constant, is determined from the time-domain data of a set of k pulses $V_k(t,z_k)$ at k = 1, 2, 3, ... different positions z_k on the line by Fourier transformation $F[V_k(t,z_k)] = |G_k(f)| \cdot e^{i\varphi_k(f)}$, with F[ ] denoting the Fourier transformation and f being the frequency. The first sampling point z_1 is taken as the origin and all the other positions are referred to z_1. Because of the time-window of 50 ps, the resolution in the frequency domain is 20 GHz. For each frequency $f_n = n \cdot 20$ GHz, n = 1, 2, 3,..., $\alpha(f_n)$ and $\beta(f_n)$ are calculated by linear regression fits to the sets of k experimental data:

$$ln|G_k(f_n)| = ln|G_1(f_n)| - \alpha(f) \cdot z_k$$
and
$$\varphi_k(f_n) = \varphi_1(f_n) - \beta(f_n)\ z_k .$$

From the phase constant $\beta(f)$, the effective permittivity $\varepsilon_{r,eff}(f) = (\frac{\beta \cdot c}{2\pi f})^2$ is calculated, with c denoting the vacuum light velocity. $\varepsilon_{r,eff}(f)$ represents a measure for the dispersion of the line: The less the slope of the function $\varepsilon_{r,eff}(f)$, the less the dispersion of the line. Subsequently, for an entirely dispersionless line, $\varepsilon_{r,eff}(f)$ is in parallel to the f axis.

RESULTS

As a first sample, a TFMSL with a 800-nm-thick SiO_2 dielectric layer deposited by plasma-enhanced chemical vapor deposition (PECVD) at 180°*C* is investigated. According to simulations by a mode-matching approach [6], the characteristic impedance is about 15 Ω. Figure 2 exhibits 5 transients from a set of pulses measured in the time-domain. The sampling positions z_k are indicated. The first pulse marked by z_1 = 0.0 mm is probed 0.5 mm away from the PC gap. Effects of finite propagation velocity, attenuation and dispersion are directly obvious from the time-domain data.

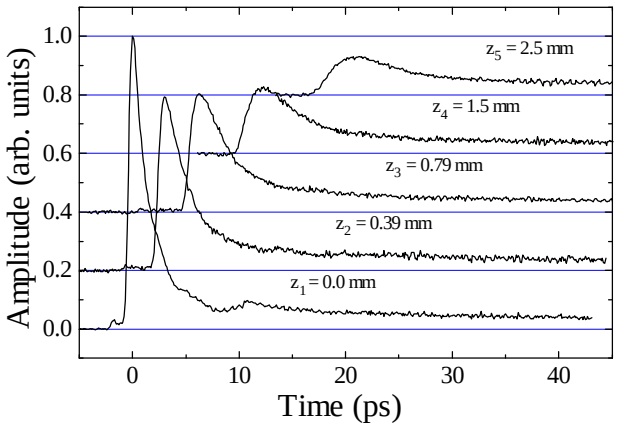

Fig. 2: Electric signals probed at various positions z_k (in mm) on the 15-Ω SiO_2-TFMSL. For clarity, the traces are shifted vertically.

With increasing propagation length, the pulses decrease in amplitude and increase in pulse width. The dip in the first transient at a delay of about 8 ps is caused by a signal reflected (with amplitude inversion) at the front edge of the $LiTaO_3$ crystal and returned from the open end of the TFMSL at the PC gap. Because of the strong attenuation this effect cannot be seen at increased propagation distances. All measured pulses show a pedestal of approximately the same height (about 4 % of the maximum of the first pulse) resulting from the smaller propagation velocities of the low-frequency components compared to the high-frequency components.

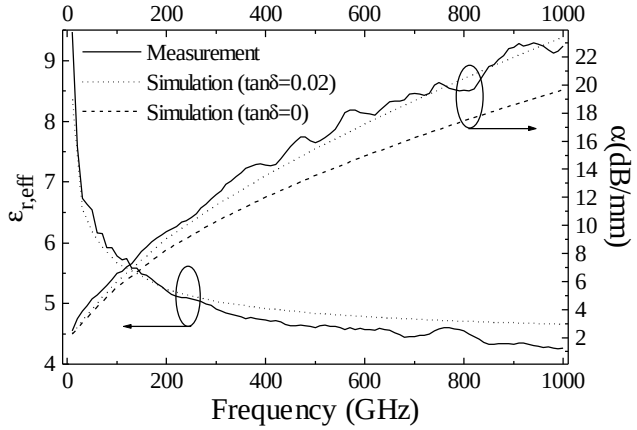

Fig. 3: Frequency dependence of the effective permittivity and the attenuation of the 15-Ω SiO_2-TFMSLs -- electrooptic measurements and full-wave simulation [3]. Al conductivity: $\kappa = 2.5 \cdot 10^7$ S/m, tanδ = 0.02, relative dielectric constant of PECVD SiO_2: ε_r = 4.9 [7].

More detailed information on attenuation and dispersion is obtained from the frequency-domain data. Figure 3 displays extracted and MoL-simulated values of both $\varepsilon_{r,eff}(f)$ and the

attenuation $\alpha(f)$ of the TFMSL as a function of frequency up to 1000 GHz. One finds unacceptably high attenuation, mainly caused by ohmic losses (α(200 GHz) ≈ 10 dB/mm). This high ohmic loss is also responsible for the significant decrease of $\varepsilon_{r,eff}(f)$ with increasing frequency, especially at lower frequencies (as known from the CPW case [6]). Up to 1000 GHz this strongly dispersive behavior, however, has no contribution from modal dispersion that would result in a distinct increase of $\varepsilon_{r,eff}(f)$ with growing frequency [1,2].

Figure 3 also shows that the measured and simulated data of both $\varepsilon_{r,eff}(f)$ and $\alpha(f)$ agree quite well. For $\varepsilon_{r,eff}(f)$, the discrepancy at the highest frequencies is about 10 %. The difference in $\alpha(f)$ between measurement and simulation for the case of tanδ = 0 can be almost eliminated assuming a frequency-independent tanδ of 0.02 or a reduced conductivity. In any case, dielectric loss of the SiO_2 material is small compared to total loss indicating that attenuation is dominated by conductor losses.

The high attenuation can be reduced significantly by increasing the thickness of the dielectric layer. Values up to 10 μm are acceptable to rule out modal dispersion below 1000 GHz. For this purpose, we used commercially available Cyclotene 3022-46 from Dow Chemicals instead of SiO_2. Cyclotene is a resin based on BCB monomers developed for inter-chip connects in multi-chip modules [8,9]. BCB monomers, dissolved in mesitylene, are spin-deposited and cured for polymerization for 60 minutes at 250°*C* in a N_2 ambient.

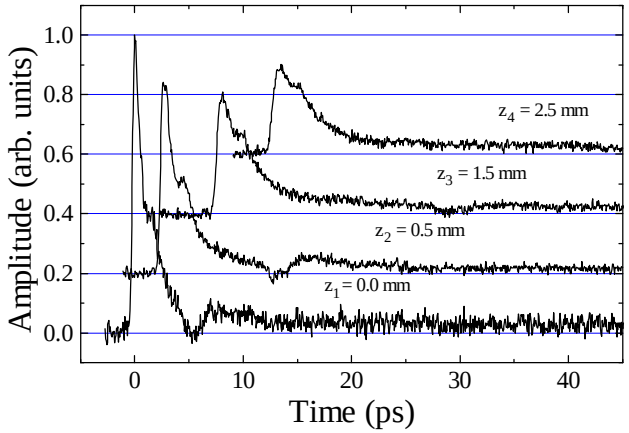

Fig. 4: Electric signals probed at various positions z_k (in mm) on the 35-Ω BCB-TFMSL. For clarity, the traces are shifted vertically.

Two TFMSLs have been fabricated with 1.7-μm-thick (spin-coating at 9000 rpm for 30 s) and 5.4-μm-thick (1000 rpm for 30 s) BCB layers, respectively. Simulations yield an impedance of 35 Ω for the 1.7 μm sample and 70 Ω for the 5.4 μm version. Figure 4 displays 4 transients from a set of signals measured on the 35-Ω BCB-TFMSL at similar positions as for the SiO_2-TFMSL. Again, the first pulse marked by z_1 = 0.0 mm is detected 0.5 mm away from the PC gap. From the time-domain data it is already obvious that the attenuation and dispersion are reduced considerably. The amplitude of the signal after 2.5 mm propagation distance is still 30 % of that of the first pulse while it is just 13 % in the SiO_2 case. The dip (compare SiO_2 data) can still be observed with the third pulse. After 1.5 mm propagation, the pulse broadening (at half maximum) is only 3.3 ps for the 35-Ω BCB-TFMSL compared to 6.1 ps for the SiO_2 line. The pedestal of the BCB line is reduced, too, so that one can expect a less pronounced decay of $\varepsilon_{r,eff}(f)$ for frequencies below 200 GHz. These statements are confirmed quantitatively by the frequency analysis of the time-domain data. Besides the experimentally determined $\alpha(f)$ and $\beta(f)$ values, Fig. 5 shows MoL simulations of the propagation constants for the two BCB lines assuming a frequency-independent loss tangent. Fitting the model at 600 GHz to the measured attenuation yields tanδ = 0.015. With this value, good agreement with the measured $\varepsilon_{r,eff}(f)$ and $\alpha(f)$ data is found throughout the entire frequency range.

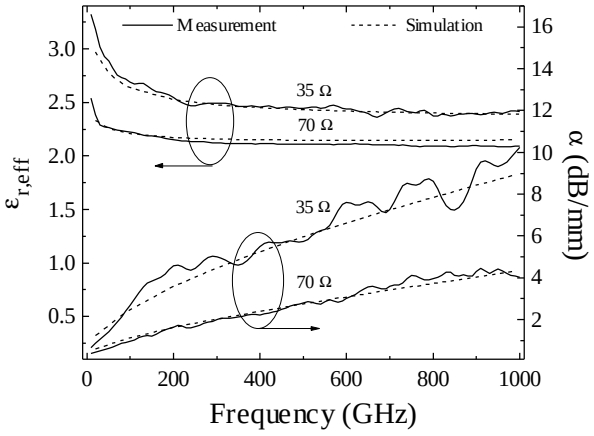

Fig. 5: Measured and MoL-simulated frequency dependence of the effective permittivity and the attenuation of two BCB-TFMSLs with insulator thicknesses of 1.7 μm (35 Ω) and 5.4 μm (70 Ω). Al conductivity: $\kappa = 2.5 \cdot 10^7$ S/m, tanδ = 0.015, relative dielectric constant of Cyclotene: ε_r = 2.7.

According to Fig. 5, the attenuation for the 35-Ω BCB-TFMSL is only about 40 % of that of the SiO_2-TFMSL. For the 70-Ω BCB-TFMSL, $\alpha(f)$ is further reduced to less than 20 % of the SiO_2 case, i.e., to approximately 4 dB/mm for the highest frequencies. The improvements in $\varepsilon_{r,eff}(f)$ are obvious from Fig. 5, too. As for the SiO_2-TFMSL, $\varepsilon_{r,eff}$ decreases monotonically with increasing frequency for both BCB lines. But in contrast to the SiO_2 line, the quantitative variation is small, and $\varepsilon_{r,eff}$ becomes almost constant for frequencies above 200 GHz. As expected, the ohmic-loss-related frequency dependence of $\varepsilon_{r,eff}$ for frequencies below 200 GHz becomes considerably weaker with increasing thickness of the dielectric. Additonally, because of the lower ε_r of 2.7 for BCB compared to SiO_2 (ε_{r,SiO_2} = 4.9), the effective permittivity is lower, resulting in higher signal velocities (0.2 mm/ps).

COMPARISON WITH CPW

In Fig. 6, the experimental and simulated data of the 70-Ω BCB-TFMSL are compared to predictions for a corresponding 70-Ω CPW on BCB. In order to reduce radiation losses and the influence of the low-resistivity Si substrate, the BCB thickness is chosen to be 25 μm. We assume a 16-μm-wide signal conductor, a slot width of 5 μm, and $\tan\delta_{BCB} = 0.015$, extracted from the experimental data of the TFMSL.

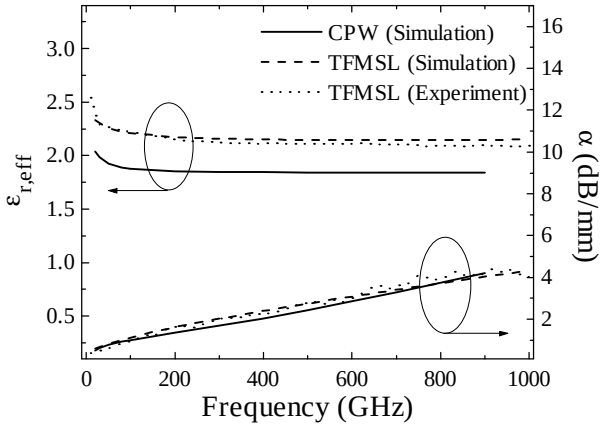

Fig. 6: Frequency dependence of effective permittivity and attenuation: comparison between the 70-Ω TFMSL of Fig. 5 (experiment and simulation) and a 70-Ω CPW on BCB (simulation). CPW geometries: 16-μm-wide center conductor, 5-μm-wide slot, 0.8-μm-thick Al metallization, 25-μm-thick BCB on low-resistivity Si.

Full-wave MoL simulations predict almost the same dispersion and attenuation for the CPW as for the TFMSL, with a somewhat lower value of $\varepsilon_{r,eff}$ for the CPW. The TFMSL, however, is more compact. A further disadvantage of the CPW on thick BCB is that the impedance is shifted towards higher values. In practice, this makes it difficult to achieve impedances of 50 Ω and lower.

CONCLUSIONS

Regarding the application in mm-wave and sub-mm-wave circuits, the following conclusions can be drawn: TFMSLs using SiO_2 as dielectric exhibit prohibitively large attenuation while TFMSLs using BCB-polymer, on the other hand, offer favorable line parameters. An almost dispersion-free behavior at moderate attenuation ($\leq$ 1 (4) dB/mm at 100 (1000) GHz)) is observed. The CPW on low-permittivity substrate shows reduced dispersion compared to conventional CPWs on semiconductor substrates, but at the expense of an increased characteristic impedance. The propagation properties of the CPWs are not superior to those of the more compact BCB-TFMSL. A particular advantage of the TFMSL is that it fully covers the common 50 Ω impedance range.

ACKNOWLEDGMENTS

The authors are grateful to Dow Chemicals for supplying free samples of Cyclotene and to R. Hey for growing LT-GaAs. This work is supported by the Deutsche Forschungsgemeinschaft (DFG) under contracts Ku 540/22 and He 1676/10.

---

a) Email: heiliger@zyklop.iht-ii.rwth-aachen.de

b) New address: Physikalisches Institut, Universität Frankfurt, Robert-Mayer-Str. 2-4, D-60054 Frankfurt

[1] H. Roskos, M. C. Nuss, K. W. Goossen, D. W. Kisker, A. E. White, K. T. Short, D. C. Jacobson, and J. M. Poate, "Propagation of picosecond electrical pulses on a silicon-based microstrip line with buried cobalt silicide ground plane", Appl. Phys. Lett. **58**, 2604 (1991).

[2] J. Gondermann, E. Stein von Kamienski, H. G. Roskos, and H. Kurz, "Al-SiO_2-Al Sandwich Microstrip Lines for High-Frequency On-Chip Interconnects", IEEE Trans. Microwave Theory Tech. **MTT-41**, 2087 (1993).

[3] R. Pregla and W. Pascher, "The Method of Lines", in *Numerical Techniques for Microwave and Millimeter Wave Passive Structures*, T. Itoh, Editor, (Wiley, New York, 1989), pp. 381- 446.

[4] E. Yablonovitch, D. M. Hwang, T. J. Gmitter, L. T. Florez, and J. P. Harbison, "Van der Waals bonding of GaAs epitaxial liftoff films onto arbitrary substrates", Appl. Phys. Lett. **56** (24), 2419 (1990).

[5] M.Y. Frankel, S. Gupta, J. A. Valdmanis, and G. A. Mourou, "Terahertz Attenuation and Dispersion Characteristics of Coplanar Transmission Lines", IEEE Trans. Microwave Theory Tech. **MTT-39**, 910 (1991).

[6] W. Heinrich, "Full-wave analysis of conductor losses on MMIC transmission lines", IEEE Trans. Microwave Theory Tech. **MTT-38**, 1468 (1990).

[7] S. M. Sze, "VLSI Technology", McGraw-Hill 1988, ISBN 0-07-062735-5, p. 259.

[8] G. M. Adema, L.-T. Hwang, G. A. Rinne, and I. Turlik, "Passivation Schemes for Copper/Polymer Thin-Film Interconnections Used in Multichip Modules", IEEE Transactions on Components, Hybrids, and Manufactoring Technology, **16** (1), pp. 53 (1993).

[9] P. B. Chinoy, and J. Tajadod, "Processing and Microwave Characterization of Multilevel Interconnects Using Benzocyclobutene Dielectric", IEEE Transactions on Components, Hybrids, and Manufactoring Technology, **16** (7), pp. 704 (1993).